The Data Acquisition System of the KOTO Experiment and RPT Upgrade

Stephanie Su, Jon Ameel, Jacqueline Beechert, Mircea Bogdan, Myron Campbell, Carolyn Gee, Margaret Huff,
Jessica Micallef, Joshua Robinson, Christopher Rymph, Hanna Schamis, Yasuyuki Sugiyama, Yasuhisa Tajima,
Monica Tecchio, Nikola Whallon, Yau Wah, and Jia Xu

***Abstract*—The KOTO experiment at J-PARC in Tokai, Ibaraki, Japan, aims to observe rare neutral kaon decay mode $K_L \to \pi^0\nu\bar{\nu}$. Followed by the first KOTO physics run in May 2013 with 24 kW beam power, we upgraded the KOTO data acquisition system in 2015 to accommodate efficient and reliable data collection with higher beam intensities.**

Lossless data compression inside the ADC modules was implemented to reduced the size of data packets. The lossless data compression enhanced the data collection rate by a factor of three. We designed a new software trigger, which consists of 47 computer nodes. It uses Infiniband hardware with MPI protocol to establish mesh network within the computer cluster and parallel data processing.

The upgrades of the KOTO data acquisition system were commissioned in 2015 and used to successfully collect data with beam intensity up to 42 kW. In preparation for increasing beam intensities in 2016 runs, we are developing the hardware trigger upgrades using the RCE Platform Technology (RPT).

I. INTRODUCTION

At the early stage of the universe, equal amounts of matter and antimatter were created. However, there is a dominance of matter over antimatter in our current universe. This phenomenon can be explained by the CP symmetry breaking. So far, experiments carried out observed insufficient CP violation to account for the CP symmetry breaking in the early universe. Therefore, studying CP violating decays can possibly discover new physics.

A. $K_L \to \pi^0\nu\bar{\nu}$

One of the famous CP violation decays is $K_L \to \pi^0\nu\bar{\nu}$, where a long-lived neutral K meson decays into neutral pion and two neutrinos. This decay is a direct CP violation and provides a clear calculation of the CP violation strength from its branching ratio. The Standard Model predicts the branching ratio BR($K_L \to \pi^0\nu\bar{\nu}$) to be $(2.4 \pm 0.4) \times 10^{-11}$ [1].

The upper limits of this branching ratio was previously measured directly and indirectly by two experiments (KEK E391a and BNL E949, respectively). The result of E391a provided a direct limit of $< 2.6 \times 10^{-8}$ at the 90% confidence level [2]. An indirect limit was derived from the Grossman-Nir bound using the results from BNL E949 to be 1.7×10^{-9} [3].

The Grossman-Nir relation is a model-independent calculation using isospin to correlate the branching ratios between $K_L \to \pi^0\nu\bar{\nu}$ and $K^+ \to \pi^+\nu\bar{\nu}$ where [4]

$$BR(K_L \to \pi^0\nu\bar{\nu}) < 4.4 \times BR(K^+ \to \pi^+\nu\bar{\nu})$$

The upper bound of BR($K_L \to \pi^0\nu\bar{\nu}$) is called the Grossman-Nir bound. Below the Grossman-Nir bound, there are many theoretical models such as Minimal Flavour Violation (MFV, [5]), Littlest Higgs model (LHT, [6]), Randall-Sundrum model (RSc, [7]), the Standard Model with four generations (SM4, [8]), and four Supersymmetry flavour models (SUSY, [9]). By probing the region below the Grossman-Nir bound, we will be able to eliminate some currently existing theoretical physics models.

Manuscript received May 30, 2016. This work was supported in part by the U.S. Department of Energy under Grant No. DE-SC0007859 and No. DE-SC0009798, the High Energy Accelerator Research Organization (KEK), the Ministry of Education, Culture, Sports, Science, and Technology (MEXT) KAKENHI No. 18071006, and the Japan Society for the Promotion of Science (JSPS) KAKENHI No. 23224007.

Stephanie Su is with the Department of Physics, University of Michigan, Ann Arbor, MI 48109 USA (e-mail: stephsu@umich.edu).

Jon Ameel is with the Department of Physics, University of Michigan, Ann Arbor, MI 48109, USA. (e-mail: sivaluna@umich.edu)

Jacqueline Beechert is with the Department of Physics, University of Michigan, Ann Arbor, MI 48109, USA. (e-mail: beechert@umich.edu)

Mircea Bogdan is with the University of Chicago, Chicago, IL 60637, USA. (e-mail: bogdan@edg.uchicago.edu).

Myron Campbell is with Department of Physics, University of Michigan, Ann Arbor, MI 48109, USA (e-mail: myron@umich.edu)

Carolyn Gee was with the Department of Physics, University of Michigan, Ann Arbor, MI 48109, USA. (e-mail: cgee@brynmawr.edu)

Margaret Huff was with the Department of Physics, University of Michigan, Ann Arbor, MI 48109, USA. (e-mail: huffm@kenyon.edu)

Jessica Micallef was with the Department of Physics, University of Michigan, Ann Arbor, MI 48109, USA. (e-mail: jessimic@umich.edu)

Joshua Robinson is with the Department of Physics, University of Michigan, Ann Arbor, MI 48109, USA. (e-mail: jorobin@umich.edu)

Christopher Rymph was with the Department of Physics, University of Michigan, Ann Arbor, MI 48109, USA. (e-mail: crymph@umich.edu)

Hanna Schamis was with the Department of Physics, University of Michigan, Ann Arbor, MI 48109, USA. (e-mail: hschamis@umich.edu)

Yasuyuki Sugiyama is with the Department of Physics, Osaka University, Toyonaka, Osaka 560-0043, Japan. (e-mail: sugiyama@champ.hep.sci.osaka-u.ac.jp)

Yasuhisa Tajima is with the Department of Physics, Yamagata University, Yamagata, Yamagata 990-8560, Japan. (e-mail: tajima@quark.kj.yamagata-u.ac.jp).

Monica Tecchio is with the Department of Physics, University of Michigan, Ann Arbor, MI 48109, USA. (e-mail: tecchio@umich.edu).

Nikola Whallon was with the Department of Physics, University of Michigan, Ann Arbor, MI 48109, USA. (e-mail: alokin@umich.edu)

Yau Wah is with the Department of Physics, University of Chicago, Chicago, IL 60637, USA. (e-mail: ywah@uchicago.edu)

Jia Xu was with Department of Physics, University of Michigan, Ann Arbor, MI 48109, USA (e-mail: jiaxu@umich.edu)

B. KOTO Experiment

The KOTO experiment is located at J-PARC in Tokai, Iabaraki, Japan. The goal of the KOTO Experiment is to observe the $K_L \rightarrow \pi^0 \nu \bar{\nu}$ decay and measure its branching ratio.

At J-PARC, the proton beam is accelerated using a 3 GeV synchrotron and further boosted by a second synchrotron to an energy of 30 GeV. The accelerated protons generate K mesons by colliding onto a gold target. These K mesons then enter and decay inside the KOTO detector. The $K_L \rightarrow \pi^0 \nu \bar{\nu}$ decay can be identified by detecting only the two photons from the π^0 decay in the final state since the neutrinos will escape from the detector. We use the Cesium Iodide (CsI) calorimeter to measure the energy and the position of the photons. Other detectors surround the CsI and serve to detect any other charged or neutral decay products and veto these decays. Due to the two missing neutrinos, our signal requires two photons with large transverse momentum deposited onto the CsI calorimeter and nothing in any of the other veto detectors as shown in Fig. 1.

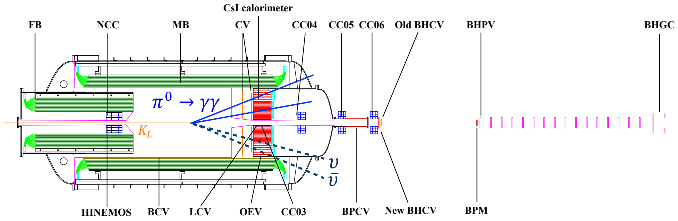

Fig. 1: Sideview of KOTO detectors. The secondary proton beam come from the left of the figure.

In May, 2013, the experiment accumulated data with $\mathrm{K_L}$ flux of 4.2×10^7 $\mathrm{K_L}$ per spill using a 2 s slow extraction of 2×10^{14} protons spill every 6 s with 24 kW beam power [10]. In 2015 runs, the proton beam power increased to 48 kW. In total, we collected about 20 times more data than in May 2013. The analysis is in progress and we intend to press the upper limit of the branching ratio below the Grossman-Nir bound. However, in order to reach the Standard Model sensitivity, higher beam intensities are required. The beam power is planned to increase up to 100 kW in the near future [11].

II. THE DAQ SYSTEM

A. Current System

Our data acquisition system consists of two types of ADC modules and three levels of triggers, as shown in Fig. 2. Two types of ADC modules, 125 MHz and 500 MHz, are used to receive PMT signals from approximately 3000 calorimeter channels and 1000 veto detector channels. The requirements for the data acquisition system are 14-bit dynamic range for the energy measurement and 1 nanosecond timing resolution. To meet these requirements, the analog PMT signals are shaped into a Gaussian waveform of $\sim$100 ns at full-width at half-maximum (FWHM) using a 10-pole Bessel filter. These waveforms are then digitized at 125 MHz or 500 MHz and recorded for each detector channel. Most of the signals generated by the detectors are digitized at 125 MHz. Detectors closed to the beam pipe generally have high signal rate; thus, the 500 MHz ADCs are used to digitize signals in these detectors. By fitting the Gaussian waveform with points 8 ns apart, we can reconstruct the timing of the PMT signals up to 1 nanosecond resolution. The timing alignment between detectors is calibrated using beam data. A lossless bit-packing data compression algorithm was implemented to enhance the data acquisition livetime.

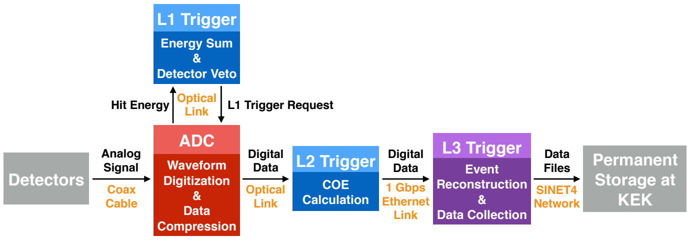

Fig. 2: The KOTO data acqsition system flow chart. The L1 trigger and the L2 trigger are hardware triggers. The L3 trigger is a software trigger. Black indicates the data being transferred. Orange represents the data link between each stage of the data acqusition system.

The trigger system contains two hardware triggers (L1, L2) and one software trigger (L3). The electronics hardware is identical for the L1 trigger and the L2 trigger, where two Xilinx FPGAs (XC5VFX70T Vertex 5 and XC4VFX12 Virtex 4) are implemented onto each electronic board. The L1 trigger only uses the functionality of the Vertex 5 FPGA and the L2 trigger uses both Vertex 5 and Vertex 4 FPGA. The data output from each ADC module is sent to the hardware triggers via 2.5 Gbps optical fibers. The ADC modules buffer the data until the L1 trigger decision is made. The L1 trigger decision is made every 8 ns by requiring a minimum total energy deposit of 550 MeV onto the CsI calorimeter and no activity in the veto detectors. Each L1 trigger module are connected to 16 ADC modules using optical fibers. The daisy-chain bus calculates the energy sum over all L1 modules and the master L1 board makes the trigger decision. The L1 trigger cut of requires a minimum 550 MeV energy deposit in the CsI calorimeter and maximum energy in other detectors, which varies based on each veto detector threshold. Upon a L1 accept, the ADC modules transmit the buffered data to the L2 trigger. Different detector trigger selections can be made and adjusted run by run. The master L1 trigger module outputs the information of detector trigger selections for each event and the data acquisition hardware trigger system performance. Prior than the June 2016 run, these information was recorded by the VME bus backplane. Trigger matching for each event was performed offline, prior for data production and analysis. In the June 2016 run, we implemented the feature of feeding these information back to an ADC module, following all the other event data stream, and be built in the L3 trigger system.

The KOTO experiment uses two characteristics from the $K_L \rightarrow \pi^0 \nu \bar{\nu}$ decay processes to identify such event - neutral decay and large transverse momentum. The veto detectors have high efficiency up to 99.9% towards detecting charged particles [12]. This eliminates other K_L decay modes such as $K_L \rightarrow \pi^+ e^- \nu_e$. Another characteristic of this neutral decay distinguishing it from all the other background K_L decays such as $K_L \rightarrow \pi^0\pi^0\pi^0$, $K_L \rightarrow \pi^0\pi^0$, $K_L \rightarrow \gamma\gamma$ is the large transverse momentum due to missing neutrinos. We implemented this characteristic onto the L2 trigger decision by weighting the energy of each CsI crystal with its own position and calculating this Center of Energy (CoE). The L2 trigger requires the CoE radius to be larger than 165 mm to distinguish our decay from other neutral decay backgrounds. Events passing the CoE cut are transmitted to the L3 trigger.

The L3 software trigger system is a computer cluster consists of 47 computer nodes. Theses computer nodes are divided into two groups, Type 1 nodes and Type 2 nodes, to receive event fragments from the L2 trigger and to rebuild complete events. Each Type 1 node has a direct connection to a L2 trigger module and receives event fragments using the Ethernet via UDP. Type 1 nodes send event fragments to Type 2 nodes for event building using the Infiniband with the MPI protocol. The Infiniband and the MPI protocol establishes intercommunication and parallel processing between computer nodes. Events are built using the the event ID and spill information contained in the data packet header and saved to the local disk. The data will later be transferred to a set of disk arrays then to the permanent storage at KEK computer server.

B. RPT Upgrade

To accommodate future increases in proton beam intensity, we are developing an upgrade for the L2 hardware trigger using the Reconfigurable Clustering Element (RCE) Platform Technology developed by SLAC. We will use the replicated mesh ATCA shelf with this RCE Platform Technology (RPT). The RPT is currently used by experiments such as ATLAS CSC, LBNE, LCLS, and LSST. We aim to implement this upgrade for the KOTO experiment runs in 2017.

A RCE has a Zynq-7030 Xilinx FPGA and a 32 GB micro SD card with linux operating system installed. The RPT we use contains a Cluster-on-Board (COB) and a Rear Transition Module (RTM). Each COB contains 9 RCEs and a Clustering Interconnect (CI), as shown in Fig. 3. The RCEs are used in different mezzanines. Eight RCEs (Zynq-7030 Xilinx FPGA) are used in the Data Processing Modules and one RCE (Zynq-7045 Xilinx FPGA) is used in the Data Transport Module. Inter data transmission between the RCEs routes through the CI.

The RTM does not contain any firmware logic. It is responsible for data receive/transmit. The data transport layout between the COB and the RTM is shown in Fig. 4.

The COB supports Rx/Tx link with input/output rate up to 120 Gbps per RCE (12×10 Gbps link). We plan to perform event reconstruction on the L2 trigger using the RCE computing power with the full inter-board connectivity provided replicated mesh ATCA backplane. A total of 6 COBs and 6 RTMs will be used.

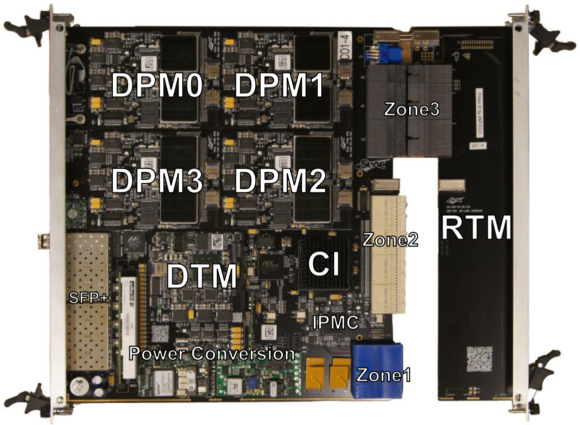

Fig. 3: Layout of a Cluster on Board (COB) and a Rear Transition Module (RTM). The COB will be inserted to the front of the ATCA crate and the RTM will be inserted from the back of the ATCA crate. Each COB contains four Data Processing Modules (DPM), one Data Transport Module (RTM), and a Clustering Interconnect (CI). Zone 1 provides the power source to the COB. Zone 2 orovides the P2 backplane connections to the ATCA crate. Zone 3 establishes the connection between the COB and the RTM [13].

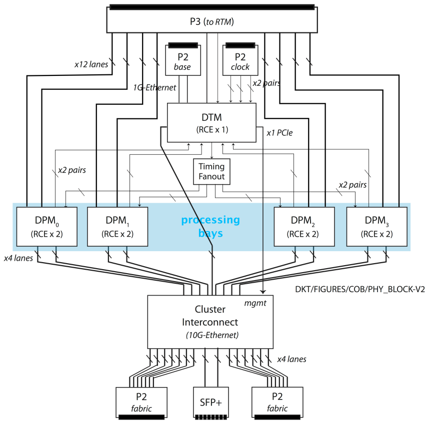

Fig. 4: The path transport of the PRT. Each RCE has 12 links to the RTM. To communicate between the RCEs within a single COB, data has to route through the CI. To communicate between inter-board RCEs, data will flow through the CI and the P2 ATCA backplane [14].

A total of eight links of the connection between a RCE and the RTM will be used to receive ADC module data and one link will be used to transmit the reconstructed event to the L3 trigger system. Each RCE will serialize the ADC packets and send it to the designated RCE via the CI and the ATCA P2 backplane for event building based on the event ID and spill information. The COE decision will be made after the event reconstruction but prior to the data transmission to the L3 trigger. Due to amount of resource available on the RCE, we are considering implementing clustering algorithm in the L2 trigger to possibility develop new data selection triggers. We are currently developing the firmware for this upgrade.

III. CONCLUSION

The current data acquisition system successfully collected data for four runs in 2015 with better performance and higher efficiency compared to 2013.

ACKNOWLEDGMENT

We express our gratitude to all J-PARC accelerator group and hadron group members who facilitated the operation of the experiment. We acknowledge KEK for providing the computer server and data storage.

We would like to thank the research group at SLAC that assisted us to learn and develop the PRT through the Department of Energy Science Graduate Student Research Program. The research is supported under Department of Energy grant No. DE-SC0007859 and No. DE-SC0009798, the High Energy Accelerator Research Organization (KEK), the Ministry of Education, Culture, Sports, Science, and Technology (MEXT) KAKENHI No. 18071006, and the Japan Society for the Promotion of Science (JSPS) KAKENHI No. 23224007.

REFERENCES

[1] J. Brod, M. Gorbahn, and E. Stamou, "Two-loop electroweak corrections for the decays," Phys. Rev. D, vol. 83, p. 034030, 2011.
[2] J. K. Ahn *et al.*, "Experimental study of the decay $K_L^0 \to \pi^0 \nu\bar{\nu}$," Phys. Rev. D, vol. 81, p. 072004, 2010.
[3] A. V. Artamonov *et al.*, "New measurement of the $K^+ \to \pi^+ \nu\bar{\nu}$ branching ratio," Phys. Rev. Lett, vol. 101, p. 191802, 2008.
[4] Y. Grossman and Y. Nir, "$K_L \to \pi^0 \nu\bar{\nu}$ beyond the standard model," Phys. Lett. B, vol. 398, p. 163, 1997.
[5] G. D'Ambrosio, G.F. Giudice, G. Isidori, and A. Strumia, "Minimal Flavour Violation: an effective field theory approach," Nucl. Phys. B, vol. 645, pp. 155-187, 2002.
[6] M. Blanke, A. J. Buras, B. Duling, S. Recksiegel, and C. Tarantino, "FCNC Processes in the Littlest Higgs Model with T-Parity," Acta Phys. Polon B. vol. 41, pp.657-683, 2010
[7] M. Blanke, A. J. Buras, B. Duling, K. Gemmler, and S. Gori, "Rare K and B Decays in a Warped Extra Dimension with Custodial Protection," JHEP, vol. 03, p.108, 2009.
[8] A. J. Buras, B. Duling, T. Feldmann, T. Heidsieck, C. Promberger, and S Recksiegel, "Patterns of Flavour Violation in the Presence of a Fourth Generation of Quarks and Leptons," JHEP, vol. 09, p. 106, 2010.
[9] W. Altmannshofer, A. J. Buras, S. Gori, P. Paradisi, and D. M. Straub, "Anatomy and Phenomenology of FCNC and CPV Effects in SUSY Theories," Nucl. Phys. B, vol. 830, p. 17, 2010.
[10] T. Masuda *et al.*, "Long-lived neutral-kaon flux measurement for the KOTO experiment," Prog. Theor. Exp. Phys, vol. 2016, p. 013C03, 2016.
[11] J. Comfort *et al.*, "Proposal for $K_L \to \pi^0 \nu\bar{\nu}$ Experiment at J-Parc", Apr. 28, 2006. [Online: http://koto.kek.jp/pub/p14.pdf]
[12] D. Naito *et al.*, "Development of a low-mass and high-efficiency charged particle detector," Prog. Theor. Exp. Phys., vol. 2016, p. 023C01, 2016.
[13] G. Thayer, "RCE Platform Technology (RPT) ATCA and the COB," RCE/ATCA Training Workshop at CERN, 2015.
[14] R. Herbst *et al.*, "Design of the SLAC RCE Platform: A General Purpose ATCA Based Data Acquisition System," SLAC-PUB-16182, 2015. [Online: http://www-public.slac.stanford.edu/sciDoc/docMeta.aspx?slacPubNumber=SLAC-PUB-16182]